The Endosomal Protein-Sorting Receptor Sortilin Has a Role in Trafficking α-1 Antitrypsin

Cristy L. Gelling,* Ian W. Dawes,† David H. Perlmutter,‡ Edward A. Fisher,§ and Jeffrey L. Brodsky[1,]*

*Department of Biological Sciences, University of Pittsburgh, Pittsburgh, Pennsylvania 15260, †School of Biotechnology and Biomolecular Sciences, University of New South Wales, Sydney, New South Wales 2052, Australia, ‡Department of Pediatrics, Cell Biology and Physiology, University of Pittsburgh School of Medicine, Children's Hospital of Pittsburgh of UPMC, Pittsburgh, Pennsylvania 15217, and §New York University School of Medicine, Division of Cardiology, Marc and Ruti Bell Program in Vascular Biology, Department of Medicine, New York, New York 10016

ABSTRACT Up to 1 in 3000 individuals in the United States have α-1 antitrypsin deficiency, and the most common cause of this disease is homozygosity for the antitrypsin-Z variant (ATZ). ATZ is inefficiently secreted, resulting in protein deficiency in the lungs and toxic polymer accumulation in the liver. However, only a subset of patients suffer from liver disease, suggesting that genetic factors predispose individuals to liver disease. To identify candidate factors, we developed a yeast ATZ expression system that recapitulates key features of the disease-causing protein. We then adapted this system to screen the yeast deletion mutant collection to identify conserved genes that affect ATZ secretion and thus may modify the risk for developing liver disease. The results of the screen and associated assays indicate that ATZ is degraded in the vacuole after being routed from the Golgi. In fact, one of the strongest hits from our screen was Vps10, which can serve as a receptor for the delivery of aberrant proteins to the vacuole. Because genome-wide association studies implicate the human Vps10 homolog, sortilin, in cardiovascular disease, and because hepatic cell lines that stably express wild-type or mutant sortilin were recently established, we examined whether ATZ levels and secretion are affected by sortilin. As hypothesized, sortilin function impacts the levels of secreted ATZ in mammalian cells. This study represents the first genome-wide screen for factors that modulate ATZ secretion and has led to the identification of a gene that may modify disease severity or presentation in individuals with ATZ-associated liver disease.

AN inherited disorder, α-1 AT deficiency (ATD) is linked to decreased levels and activity of the proteinase inhibitor α-1 antitrypsin (AT). It is one of the most common genetic disorders in the United States, with the most severe form affecting between 1 in 3000 and 1 in 6000 individuals (Kimpen *et al.* 1988; Silverman *et al.* 1989; Spence *et al.* 1993; de Serres *et al.* 2007, 2010).

Wild-type AT (referred to here as the M variant, or ATM) is an abundant plasma protein secreted by hepatocytes that protects lung tissue from the action of neutrophil elastase. The most common cause of ATD is homozygosity for the mutation that gives rise to the Z variant of AT (ATZ), which exhibits folding and thus secretion defects. Retention of ATZ within hepatocytes results in AT deficiency in the lungs—considered a loss-of-function phenotype—but can also result in an accumulation of polymeric and aggregated ATZ within the liver, which manifests as a gain-of-function phenotype (Bathurst *et al.* 1984, 1985; Foreman *et al.* 1984; Errington *et al.* 1985; Janus *et al.* 1985; Perlmutter *et al.* 1985a,b; Dycaico *et al.* 1988; Carlson *et al.* 1989; Lomas *et al.* 1992). These organ-specific effects of ATZ are consequently responsible for the two most common clinical manifestations of ATD, lung disease and liver disease.

Interestingly, there is considerable variability in the age-of-onset and severity of these diseases, particularly in the case of liver disease associated with ATD. For example, only ~12% of infants that are homozygous for ATZ develop clinically significant liver dysfunction (Sveger 1976), suggesting that genetic and environmental factors modify the risk and severity of early childhood liver disease. In addition, an autopsy study of 94 ATZ homozygous patients found that 37% had cirrhosis and 15% had primary liver cancer, indicating that risk for ATD-associated liver disease is also variable in

doi: 10.1534/genetics.112.143487
Manuscript received July 2, 2012; accepted for publication August 17, 2012
Supporting information is available online at http://www.genetics.org/lookup/suppl/doi:10.1534/genetics.112.143487/-/DC1.
This paper is dedicated to the memory of Cameron Peterson (1988–2011).
[1]Corresponding author: Department of Biological Sciences, A320 Langley Hall, University of Pittsburgh, Pittsburgh, PA 15260. E-mail: jbrodsky@pitt.edu

adults (Eriksson 1987). To date, the identities of the factors that modify the risk for ATD-associated liver diseases remain unknown. One difficulty with identifying these modifiers may be that the effects will be subtle; *e.g.*, small changes in secretion or degradation efficiency may become magnified and pathologically relevant only after long periods of time.

A correlation between ATZ degradation and ATD-associated liver disease was first supported by the finding that fibroblasts from ATD patients with liver disease showed a lag in the degradation of transduced ATZ compared to fibroblasts from ATD patients without liver disease (Wu *et al.* 1994). Consistent with this hypothesis, a candidate gene-sequencing study of endoplasmic reticulum (ER) mannosidase I (ERManI), which facilitates the degradation of misfolded secreted proteins (Hosokawa *et al.* 2003; Wu *et al.* 2003), suggested that differences in ERManI expression are associated with earlier age-of-onset of end-stage liver disease (Pan *et al.* 2009). However, because of the small number of samples available for study, the significance of this association has been challenged (Chappell *et al.* 2009; Pan and Sifers 2009). Even if the ERManI polymorphism does not prove to be a clinically significant modifier of ATD, there are likely to be many other factors that modify ATD-associated liver disease.

We have proposed that one way to identify candidate genetic modifiers of ATD-associated liver disease is to take advantage of the genetic and genomic methods available for the bakers' yeast *Saccharomyces cerevisiae* (Gelling and Brodsky 2010). In theory, mutant screens might be used to identify conserved genes that affect the disease-associated properties of ATZ expressed in yeast. Indeed, previous work on ATZ in yeast has supported several key insights into the mechanisms of ATZ degradation that have been confirmed by experiments in mammalian cells. For example, ATZ was among the first substrates shown to be degraded by the proteasome via a process known as ER-associated degradation (ERAD) (Qu *et al.* 1996; Werner *et al.* 1996). Studies in yeast were also the first to establish that the ER lumenal chaperone BiP plays an important role in the ERAD of ATZ (Brodsky *et al.* 1999; Cabral *et al.* 2002; Schmidt and Perlmutter 2005).

In addition to ERAD, another mechanism for degradation of misfolded or aggregation-prone ER proteins is autophagy. In the canonical pathway, cytoplasmic cargo destined for autophagic degradation is encapsulated within double-membrane vesicles and is then transported to the lysosome (the vacuole in yeast). That ATZ can also be degraded by autophagy was demonstrated in yeast, mouse embryonic fibroblasts, and mice (Teckman and Perlmutter 2000; Kamimoto *et al.* 2006; Kruse *et al.* 2006). It is currently unknown whether ATZ that is targeted for autophagy has been retrotranslocated from the ER into the cytoplasm, where it may aggregate, or whether the protein is degraded directly via "ER-phagy" (Bernales *et al.* 2006; Yorimitsu *et al.* 2006). Regardless, consistent with a contribution of autophagy to ATZ clearance, an anti-epileptic drug that induces autophagy was found to decrease liver damage in an ATZ mouse model (Hidvegi *et al.* 2010).

Data from the yeast model has also suggested that ATZ might traffic to the vacuole/lysosome via the secretory pathway (Kruse *et al.* 2006), a hypothesis that has not yet been investigated in mammalian systems. Since our previous approaches to pathway identification were relatively targeted (Palmer *et al.* 2003), we reasoned that a more comprehensive picture of ATZ degradation would be gained by use of the yeast genome-wide deletion mutant collection (Giaever *et al.* 2002), which includes mutants for each nonessential gene. Among these are mutants with specific defects in ERAD, autophagy, the secretory pathway, as well as other degradative pathways and protein quality control mechanisms.

In this article, we describe a new yeast AT expression system that allowed us to screen the yeast deletion mutant collection for strains with increased intracellular accumulation and secretion of ATZ. This screen revealed that mutations that impair endosomal sorting to the vacuole result in increased secretion of ATZ. Indeed, one of the strongest hits from our screen was *vps10*Δ [sortilin (Sort) in mammals], which has been suggested to aid in the selection and delivery of misfolded Golgi proteins to the vacuole (Hong *et al.* 1996). Using a mammalian ATZ expression system, we then found that sortilin also impacts ATZ accumulation and secretion. Together, our evidence supports a model in which a portion of ATM and ATZ is degraded in the vacuole/lysosome after trafficking through the Golgi in both yeast cells and mammalian cell culture.

Materials and Methods

Yeast strains and culture conditions

BY4742 (Brachmann *et al.* 1998) was used as the wild-type yeast strain in all experiments. All mutant strains were derived from the haploid α-mating-type *S. cerevisiae* deletion mutant collection (Winzeler *et al.* 1999) obtained from Invitrogen, except for BY4742 *atg14Δ*, which was made by transformation of BY4742 with an *ATG14*::*KanMX* cassette that was PCR-amplified from genomic DNA of the strain BY4741 *atg14Δ* (Invitrogen) using the primers 5′-AAAGGT TATCTTTTAAAGCCGCTAA-3′ and 5′-ATTTATGGCAAACA ACTCCTTATCA-3′. The identities of the *pep4Δ*, *atg14Δ*, *vps10Δ*, and *vps30Δ* strains were confirmed by PCR. Yeast were cultured at 30° in all experiments, standard growth media formulations were used (Adams *et al.* 1997), and cultures at an OD_{600} of 0.4–0.9 were considered to be in log phase. Plasmids were introduced into cells by lithium acetate transformation (Gietz *et al.* 2002). For induction of expression from the *MET25* promoter, yeast transformants were cultured in synthetic complete medium lacking uracil and methionine (SC−ura−met) for the indicated times.

Plasmid construction

The yeast expression plasmids pATM-GFP and pATZ-GFP were constructed using the AT-GFP fusion cassettes from a set of mammalian AT expression constructs. These

cassettes consisted of the human ATM- or ATZ-coding sequence fused at the C terminus with enhanced GFP (eGFP) derived from pEGFP-N1 (Clontech). A Kozak sequence (CCACC) was inserted immediately upstream of the start codon of the fusion cassette, and a 15-bp linker of vector-derived sequence separated the last codon of AT from the start codon of eGFP (amino acid sequence: GPVAT). These fusion cassettes were PCR-amplified using the primers 5′-GGAATTCGCTAGCCCACCATG-3′ and 5′-CCTCGAGCGC GGCCGCTTTACTT-3′ (restriction sites underlined). The amplicons were digested with *Eco*RI and *Xho*I and then cloned into the yeast expression vector pRS423MET25 (Mumberg *et al.* 1994).

AT yeast expression plasmids lacking eGFP were constructed from pATM-GFP and pATZ-GFP by introducing a stop codon at the end of the AT ORF by PCR amplification with the primers 5′-CCTTCGTGTAATACAGGGTCGTC-3′ and 5′-CATGACTCGAGTTACTATTTTTGGGTGGGATTCAC CAC-3′ (restriction site underlined). This untagged AT cassette was cloned into pRS426MET25 (pATM and pATZ) or pRS423MET25 (pATM-2 and pATZ-2) using the *Eco*RI and *Xho*I restriction sites.

Mammalian expression constructs bearing ATM and ATZ fused with a FLAG epitope and a tetracysteine (TC) tag at the C terminus were generated using two rounds of PCR followed by restriction enzyme digestion and ligation. The first round of PCR introduced the FLAG tag, while the second round introduced the TC tag. The first round of PCR was performed using the primers 5′-GCCACCATGCCGTCTT CTGTCTCG TG-3′ and 5′-AACAGTTCAAGAACTTATCGTC GTCATCCTTGTAATCTTTTTGGGTGGGATTCACCACTT-3′. The Kozak sequence is underlined. The templates used for the first round of PCR amplification were the ATM and ATZ constructs in the pRc/RSV vector (Invitrogen) that were described in Lin *et al.* (2001). The resultant PCR products were used for the second round of PCR amplification using the primers 5′-GGGAAGCTTGCCACCATGCCGTCT TC-3′ and 5′-CCCGCGGCCGCTTAAGGC TCCATGCAACAGCCAGGACAAC AGTTC AAGAACTTATCGTCG-3′, which contained the *Hin*dIII and *Not*I restriction enzyme sites, respectively (underlined). The resulting PCR amplicons were subcloned into the *Hin*dIII and *Not*I sites of pRc/RSV. The identity of all constructs was confirmed by restriction digestion and DNA sequencing.

Immunoblot analysis

Yeast cell lysates were prepared using a modification of an alkaline/detergent lysis method (von der Haar 2007). Briefly, cells were harvested and resuspended in lysis buffer (0.1 M sodium hydroxide, 0.05 M EDTA, 2% SDS, 2% 2-mercaptoethanol) and then incubated at 90° for 10 min. The mixture was neutralized with an equal volume of 0.2 M acetic acid containing 2% 2-mercaptoethanol and incubated for an additional 10 min at 90°. Cell lysates were resolved by SDS-PAGE, and total protein was transferred to nitrocellulose membranes for immunoblot analysis.

The following antibodies were used for immunoblot analysis: rabbit anti-human AT (Dako); rabbit anti-yeast glucose-6-phosphate dehydrogenase (Sigma); rabbit anti-yeast BiP (Brodsky and Schekman 1993); rabbit anti-yeast carboxypeptidase Y (CPY) (Abcam); rabbit anti-yeast Sec61 (Stirling *et al.* 1992); rabbit anti-GFP (S. Subramani, University of California, San Diego). Primary antibody was detected with donkey HRP-conjugated anti-rabbit IgG secondary antibody (GE Healthcare). HRP signal was detected with Supersignal West Pico or Supersignal West Femto Chemiluminescent Substrate (Pierce) and imaged with a Kodak Image Station 440 *CF*.

Cell fractionation and protease protection

For separation of cell lysates into soluble and membrane fractions, cells were grown to log phase in SC−ura−met, harvested, and converted to spheroplasts by treatment with lyticase. Spheroplasts were overlaid onto a solution containing 0.8 M sucrose, 1.5% Ficoll 400, and 20 mM HEPES, pH 7.4, and centrifuged at 6000 × *g* for 10 min at 4° before being resuspended in ice-cold buffer 88 (20 mm HEPES, pH 6.8, 150 mM KOAc, 250 mM sorbitol, 5 mM MgOAc, 1 mM DTT, 2 mM PMSF, 0.5 μg/ml pepstatin A, and 1 μg/ml leupeptin) and lysed with 20 strokes in a Dounce homogenizer. Unbroken cells and debris were removed by centrifugation at 500 × *g* for 5 min at 4°, and the clarified lysate was centrifuged again at 18,000 × *g* for 25 min. The supernatant and pellet fractions were examined by immunoblot analysis as described above.

For protease protection assays, ER-enriched microsomes were prepared as previously described (Brodsky *et al.* 1993). Microsomes were treated at 4° for 30 min with 4 mg/ml trypsin in buffer 88, with 4 mg/ml trypsin and 1% triton X-100 in buffer 88, or with buffer 88 alone. Treatment was stopped by precipitation with trichloroacetic acid to a final concentration of 25%, and immunoblot analysis was performed as described above.

Immunofluorescence and live-cell microscopy

Immunofluorescence was performed using a modification of a described method (Amberg *et al.* 2005). Briefly, cells were grown to log phase in SC−ura−met and fixed for 1 hr in 4% formaldehyde. Fixed cells were washed and then converted to spheroplasts by treatment with zymolyase (US Biological). The fixed spheroplasts were attached to polylysine-treated microscope slides and permeabilized by methanol treatment. The slides were blocked with 0.5% BSA and 0.5% ovalbumin and then stained with rabbit anti-human AT (Dako) and mouse anti-yeast BiP (M. Rose, Princeton University), followed by staining with Alexa Fluor 488 goat anti-rabbit IgG and Alexa Fluor 647 goat anti-mouse IgG (Invitrogen). The slides were mounted with Prolong Antifade Gold containing DAPI (Invitrogen) and imaged with a Leica TCS SP5 confocal microscope (Figure 1B) or with a Olympus FV1000 fluoview confocal microscope (Figure 4A).

Live-cell fluorescence imaging of yeast expressing AT-GFP (pATM-2 or pATZ-2) and a Sec63-mCherry fusion (pBK177, obtained from J. Frydman, Stanford University) was performed after growth of the culture to log phase in SC−ura−met. Cells were harvested and resuspended in fresh medium before being immobilized onto a polylysine-coated coverslip by overlaying with a slab of 1% agarose. Cells were imaged on an inverted Zeiss Meta 510 confocal fluorescence microscope.

Colony immunoblot assay and genetic screen

To assay AT secretion by yeast colony immunoblot, cells expressing AT were spotted onto nitrocellulose, which was then overlaid on SC−ura−met agarose medium. After 14–16 hr of growth at 30°, the cells were rinsed from the nitrocellulose with distilled water and then immunoblotted for AT as described above and in Kruse *et al.* (2006). To assay total intracellular and secreted AT levels by colony immunoblot, the same procedure was performed, except before being rinsed from the membrane the cells were lysed *in situ* for 30 min in 0.2 M NaOH, 0.1% SDS, and 0.05% 2-mercaptoethanol (McCracken *et al.* 1996).

To screen for yeast mutant strains with altered AT expression or secretion, the haploid α-mating-type (BY4742) *S. cerevisiae* deletion mutant collection (Winzeler *et al.* 1999) was obtained from Invitrogen, and the plasmid pATZ was introduced into each strain by lithium acetate transformation (described above). Transformants were selected by plating on solid SC−ura containing 1 mM methionine to repress expression of ATZ. Transformants were transferred to liquid SC−ura plus 1 mM methionine and grown at 30° in a humidified chamber for an additional 3 d. The cells were then spotted onto nitrocellulose membranes using a 96-pin blot replicator (V&P Scientific), and the membranes were overlaid on solid SC−ura−met. After 15 hr of growth at 30°, the membranes were processed for colony immunoblot analysis as described above. The immunoblot signal was quantified by taking the pixel intensity from each spot and subtracting the background value from an empty well. In the primary screen, the signal for each strain was then normalized to the mean value for all viable strains on the same plate. In the secondary screen, the corrected signal was normalized to a paired wild-type control (*i.e.*, a wild-type control in the adjacent well).

Yeast pulse-chase analysis

Yeast cells were grown to log phase in SC−ura−met and then harvested and resuspended in the same medium at an OD_{600} of 5. The cells were incubated for 20 min at 30°, and then EasyTag Express ^{35}S protein labeling mix (PerkinElmer NEN) was added to a final concentration of 100 μCi/mL. The cells were labeled at 30° for 5 min before the incorporation of radioactive amino acids was quenched by the addition of 5 mM methionine and 2 mM cysteine. Cells were harvested at the indicated times, and the cell pellets were flash-frozen in liquid nitrogen. Cell extracts were prepared by glass-bead disruption in 50 mM Tris–Cl (pH 7.4), 1% SDS, 1 mM EDTA, plus 1 mM PMSF, 0.5 μg/ml pepstatin A, and 1 μg/ml leupeptin. Extracts were cleared by centrifugation at 15,000 × *g* for 10 min at 4°, and total incorporated radiolabel in the supernatant was assessed by liquid scintillation counting. AT was immunoprecipitated from the cell extracts using rabbit anti-human AT (Dako) coupled to AffiGel 10 matrix (Bio-Rad) and eluted by incubating in SDS-PAGE sample buffer at 90° for 5 min. Immunoprecipitates were separated by SDS-PAGE, fixed, dried, and visualized by phosphorimager analysis on a Typhoon FLA 7000 (GE).

Cycloheximide chase analysis

BY4742 wild-type and *atg14Δ* cells expressing ATM or ATZ were grown to log phase in SC−ura−met before being harvested and resuspended at an OD_{600} of 1. Cells were incubated with shaking at 30° for 20 min before a sample was taken as the zero time point. Cycloheximide was added to a final concentration of 75 μg/ml, and then additional samples were taken at the time points indicated. AT levels were examined by immunoblot analysis as described above.

Autophagy assays

BY4742 wild-type, *vps10Δ*, and *atg14Δ* cells were transformed with pGFP-Atg8 (D. Klionsky, University of Michigan) and grown to log phase in SC−ura−met. The culture was split, one sample was harvested as a control ("+ nitrogen source"), and the remainder was washed and resuspended in SD lacking amino acids and ammonium sulfate. This culture was incubated at 30° for 4 hr before being harvested ("− nitrogen source"). Cell lysates were prepared and assessed by immunoblot analysis as described above.

Pulse-chase analysis in rat hepatoma cells

The generation of rat hepatoma McA-RH7777 cells stably overexpressing apolipoprotein B and either wild-type sortilin or mutant sortilin—in which key residues in the dileucine and tyrosine endosomal sorting motifs are mutated to alanine (Sort.LAYA)—was recently described (Strong *et al.* 2012). These cells were cultured at 37°, 5% CO_2, in Dulbecco's Modified Eagle's Medium (DMEM) supplemented with 10% fetal bovine serum, 10% horse serum, L-glutamine, and penicillin/streptomycin. Cells were transfected with pRC/RSV-ATM-FLAG-TC, pRC/RSV-ATZ-FLAG-TC, or the vector control pRC/RSV using Lipofectamine 2000 according to the manufacturer's instructions (Invitrogen). After 24 hr, the cells were pretreated for 20 min with DMEM lacking cysteine and methionine and then labeled with 100 μCi EasyTag Express ^{35}S protein labeling mix (Perkin-Elmer NEN) for another 20 min. The cells were washed with chase medium (DMEM supplemented with 5 mM cysteine, 5 mM methionine, and 10 mM HEPES buffer at pH 7.4) and were then incubated in chase medium for an additional 20 min. The cells were placed on ice, the medium was harvested,

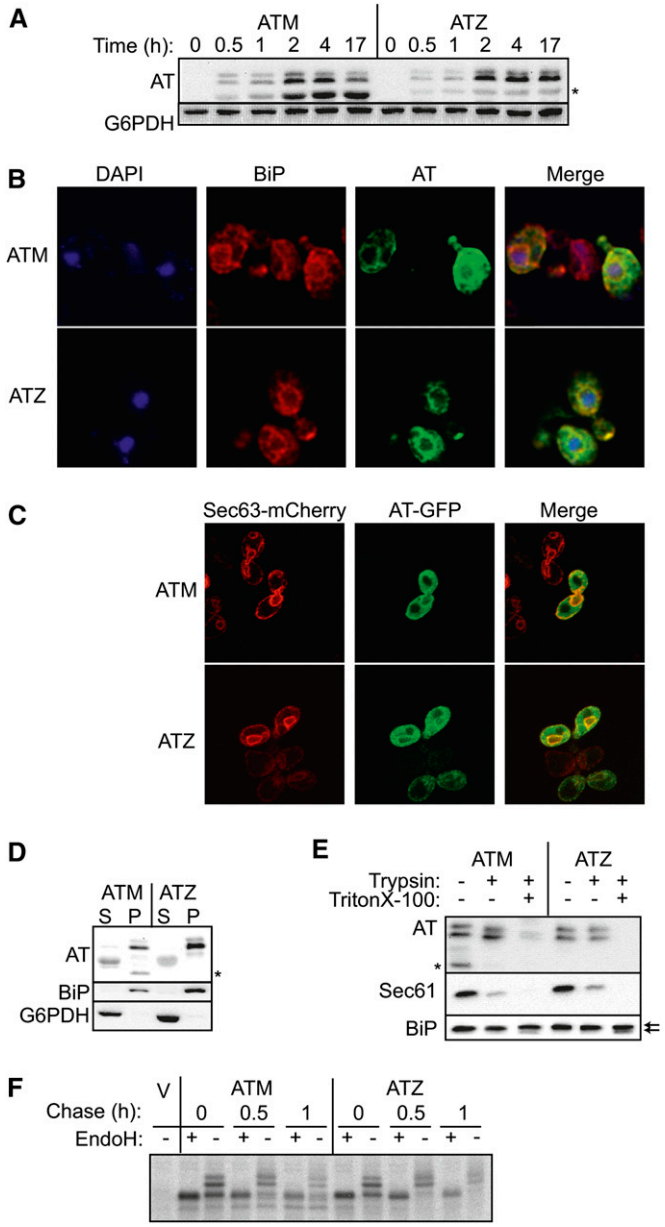

Figure 1 Human AT expressed in yeast resides primarily in the ER. (A) ATM and ATZ expression in wild-type yeast was induced by transfer of transformed cells to growth medium lacking methionine. Cell extracts were taken at the indicated times and AT levels were assayed by immunoblot. G6PDH was used as a loading control. The two top bands represent the ~55- and 53-kDa species. (B) Indirect immunofluorescence microscopy of BiP and AT indicates that ATM and ATZ are primarily localized to the ER (visible as a perinuclear ring). The relative location of the nucleus is shown by DAPI staining. (C) Live-cell fluorescence microscopy of AT-GFP and Sec63-mCherry supports the ER residence of ATM and ATZ. (D) To determine whether ATM and ATZ reside within a membrane compartment, cell lysates were separated into an ER-membrane-enriched pellet fraction (P) and a nonmembrane supernatant (S), and levels of AT, the ER lumenal protein BiP, and the cytosolic protein G6PDH were assayed by immunoblot. (E) ER-enriched microsomes were incubated in the presence or the absence of trypsin and TritonX-100 as indicated, and the levels of AT, BiP, and the ER membrane protein Sec61 were assayed by immunoblot. Arrows indicate the position of the doublet that indicates an intermediate BiP degradation product formed after trypsin treatment. (F) A pulse-chase analysis was used to establish *N*-linked glycosylation of AT. ^{35}S-labeled-AT was immunoprecipitated and treated with either Endo H or incubated with buffer before being analyzed by SDS-PAGE. "V" indicates vector control samples (which lack AT). In Figures 1 and 2 an asterisk indicates an AT species that was not found within the ER lumen.

and the cells were lysed in a buffer containing 50 mM Tris–Cl, pH 8, 100 mM EDTA, 0.4% deoxycholate, 1% NP40, 2 mM PMSF, and 1× complete protease inhibitor cocktail (Roche). Cell lysates and media were clarified by centrifugation at 500 × *g* for 10 min at 4° before an immunoprecipitation analysis was performed with either anti-FLAG M2 affinity gel (Sigma) or goat anti-human α-1 AT (Diasorin) coupled to AffiGel 10 matrix (Bio-Rad) at 4° overnight. Immunoprecipitates were analyzed by SDS-PAGE as described above for the yeast pulse-chase analysis.

Statistical analysis

To identify statistically significant differences between AT levels in wild-type and *pep4Δ* mutants (Figure 4C), two-tailed *t*-tests were performed. To test whether AT levels were different between McArdle RH-7777 cells expressing Sort and those expressing Sort.LAYA, the AT signal from five replicates were log-transformed to allow for the use of a paired, two-tailed *t*-test. Statistically significant Gene Ontology enrichments in the list of mutants with increased ATZ secretion were determined from the YeastMine interface of the *Saccharomyces* Genome Database (http://yeastmine.yeastgenome.org). In our case, comparisons were made using the hypergeometric distribution incorporating a Benjamini–Hochberg multiple testing correction.

Results

Human AT localizes to the yeast ER

To identify factors that modulate ATZ biogenesis in a genome-wide deletion screen, we modified an existing yeast AT expression system (McCracken and Kruse 1993). The galactose-inducible system used in previous work required a lengthy and physiologically stressful induction procedure, and the AT expression levels achieved in this way were often low. To address these shortcomings, the *MET25* methionine-repressible promoter was used to drive plasmid-based expression of the human wild-type AT (ATM), and the disease-associated variant (ATZ). AT expression from the *MET25* promoter was greater than that achieved with the galactose-inducible system (data not shown), and expression was rapidly induced upon removal of methionine from the medium (Figure 1A). AT expressed using this system consisted of three species: the two slower-migrating species corresponded to translocated, glycosylated AT, while the faster-migrating species (indicated with an asterisk) likely corresponds to an unglycosylated, incomplete translocation product (see below).

ATM is a secreted protein, but within the cell it is primarily localized to the ER (Lin *et al.* 2001), where it is folded and post-translationally modified. ATZ is inefficiently secreted and the majority is retained in the ER (Carlson *et al.* 1989; Lin *et al.* 2001). Therefore, we expected to find that AT expressed in yeast would also reside primarily in the ER. As anticipated, ATM and ATZ expressed using the *MET25* system were shown by immunofluoresence to significantly colocalize with the ER lumenal chaperone BiP (Figure 1B). Consistent with ER localization, C-terminal GFP fusions of ATM and ATZ partially colocalized with the ER-membrane marker Sec63-mCherry (Figure 1C). Areas in which colocalization was not evident most likely represent fractions of AT that had trafficked beyond the ER or the poorly translocated fraction.

To confirm that the ER-associated AT resided in the ER lumen, cell lysates were separated into an ER-enriched membrane fraction and a soluble supernatant. Consistent with the hypothesis that a portion of AT is poorly translocated, the soluble fraction contained an AT species of ~47 kDa, which is similar to the expected size of unprocessed precursor AT (*i.e.*, including the signal sequence) (Figure 1D). However, the majority of AT was found as an ~53-kDa species in the membrane fractions, which is similar to the molecular mass of the intracellular, glycosylated form of AT observed in mammalian cells. In addition to the ~53-kDa species, the membrane fraction contained a larger species, of ~55 kDa, and a smaller species of the size predicted for processed, but unglycosylated, AT (~44 kDa; see asterisk).

The ~53- and ~55-kDa species were protected from protease digestion, which, together with the ER localization, indicated that these species resided in the ER lumen (Figure 1E). Furthermore, these species showed increased electrophoretic mobility after endoglycosidase H (Endo H) treatment, which indicates that they were modified by *N*-glycosylation in the ER (Figure 1F). It should be noted that, in contrast to the case for mammalian glycoproteins, yeast *N*-glycoproteins remain Endo H-sensitive in all compartments of the endomembrane system.

In contrast, the ~44-kDa species from the membrane fraction (indicated by an asterisk in Figure 1, A, D, and E) was sensitive to protease digestion and was not *N*-glycosylated, suggesting peripheral association with the ER. This species may represent a stalled translocation product of AT and was excluded from subsequent analysis. Interestingly, a greater proportion of this form was found for ATM compared to ATZ. If this product is indeed an incomplete translocation product, then the difference between the ATM and ATZ variants might reflect differences in surveillance and protein degradation by cytoplasmic quality control pathways, since it was more rapidly degraded when observed in ATZ- than in ATM-expressing cells (not shown). Nevertheless, these data confirm that a significant proportion of ATM and ATZ is translocated into the yeast ER.

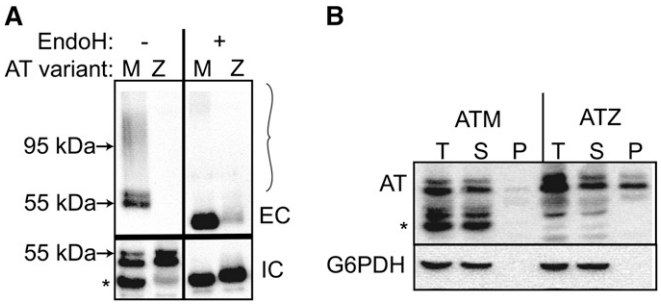

Figure 2 ATZ is less efficiently secreted and is less detergent-soluble than ATM. (A) Wild-type yeast expressing ATM (M) or ATZ (Z) were grown to log phase and cell lysates (intracellular; IC) and conditioned media (extracellular; EC) were prepared and treated in the presence (+) or the absence (−) of Endo H before being analyzed by immunoblot. The large brace indicates high-molecular-weight species corresponding to hyperglycosylated AT. Arrows indicate the positions of the 95- and 55-kDa molecular mass standards for comparison of the EC and IC species. (B) ATM- or ATZ-expressing cells were converted to spheroplasts and were lysed with Triton X-100. The extracts were then separated into total (T), soluble (S), and insoluble (P) fractions by centrifugation, and AT and the soluble protein G6PDH were analyzed by immunoblot.

ATZ characteristics associated with the disease state are recapitulated in yeast

Most ATZ-associated lung disease likely arises from the significant decrease in the amount of ATZ that is secreted from hepatocytes compared to ATM. Therefore, the comparative secretion efficiencies of the ATM and ATZ variants in yeast were assessed by immunoblot analysis of conditioned media. ATM but not ATZ was detectable in the media (EC), with a significant proportion of ATM present as a series of high-molecular-weight species (Figure 2A, left). This "smear" is commonly observed for secreted yeast proteins (*e.g.*, Esmon *et al.* 1981) and typically reflects extension of *N*-glycans in the Golgi, referred to here as hyper *N*-glycosylation. We hypothesized that, if secreted ATZ were also subject to hyper *N*-glycosylation, the effect of "smearing" the ATZ immunoblot signal would decrease overall signal intensity, making it difficult to detect secreted ATZ. Indeed, after Endo H treatment, a small amount of secreted ATZ was detectable (Figure 2A, right). However, even after Endo H treatment, ~10-fold less ATZ was present in the secreted fraction compared to ATM. This was not due to significant portions of ATZ being trapped in the periplasm, since treatment of cells with zymolyase did not result in the liberation of additional extracellular material (not shown).

In addition to this secretion defect, the ATZ variant was partially insoluble in the presence of a mild detergent (Figure 2B), as is the case for ATZ expressed in mammalian cells (Lin *et al.* 2001). Only a negligible amount of ATM was found in the pellet after Triton X-100 treatment, whereas a significant fraction of ATZ remained insoluble under identical conditions.

Overall, these results indicated that AT variants expressed in yeast recapitulate two important characteristics associated with AT expression in mammalian cells. First, ATM is

secreted more efficiently than ATZ, and, second, a greater proportion of ATZ is found in a Triton X-100-insoluble fraction.

Development of a colony immunoblot assay to monitor secreted and total AT levels

To date, a whole-genome analysis to identify genetic modulators of ATZ secretion has not been undertaken. Our hypothesis was that "hits" from this analysis might include candidate genetic modifiers of ATD and new therapeutic targets.

To screen for yeast mutants that affect ATZ secretion, it was first necessary to develop an AT secretion assay suitable for a microplate format so that the yeast deletion mutant collection could be analyzed. The method chosen was colony immunoblot assay, in which yeast cells are spotted onto a nitrocellulose membrane and the membrane is then overlaid on growth medium. In our case, after overnight growth, the cells were rinsed from the membrane, and AT captured by the membrane was analyzed by immunoblot. As shown in Figure 3A, secreted ATM was readily detected using this method, while an intracellular control [glucose-6-phosphate dehydrogenase (G6PDH)] was absent from the media (EC). This indicates that the AT signal was not due to cell lysis (Figure 3A, left). Using this method, we could also recapitulate the difference in secretion efficiency between ATM and ATZ that was evident in conditioned media (Figure 2A). In addition, we were able to detect a threefold increase in ATZ secretion in a *vps30Δ* mutant, which is required for both autophagy and CPY-to-vacuole targeting via the Golgi, and was previously shown to impact the secretion and stability of ATZ (Kruse *et al.* 2006).

Through a modification of the colony immunoblot procedure we were also able to assay the steady-state intracellular and cumulative extracellular levels of AT. Specifically, a high-pH, SDS lysis step was added immediately before the yeast cells were rinsed from the membrane (referred to hereafter as a lysed colony immunoblot). Immunoblotting for the intracellular control G6PDH indicated that an intracellular protein could be detected using this method (Figure 3A, right). The use of lysed colony immunoblots also demonstrated that the ATZ secretion defect was not an artifact of poor ATZ expression, since the difference between ATM and ATZ signal intensity was much smaller when the lysis step was included than when only secreted AT was assayed (compare M and Z spots in EC *vs.* intracellular (IC) + extracellular (EC) panels of Figure 3A and the quantified data from three independent experiments in Figure 3B).

These methods were further validated by using the same procedure to detect secreted and total levels of the vacuolar protein CPY. In wild-type cells, CPY is almost entirely intracellular, and in a *vps30Δ* mutant, CPY is robustly secreted, with relatively little retained in the cell (Robinson *et al.* 1988). As anticipated, the CPY secretion phenotype of a *vps30Δ* mutant was evident in unlysed colony immunoblots

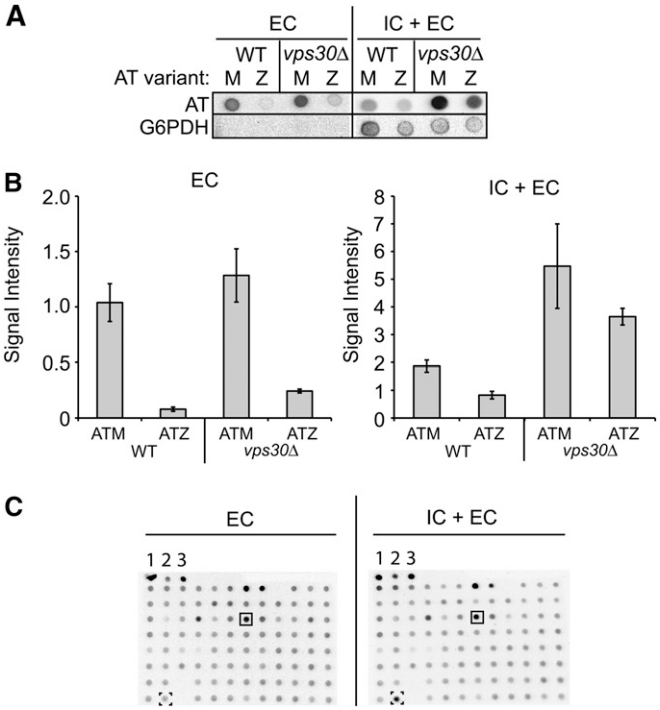

Figure 3 ATZ levels and secretion can be assayed by colony immunoblot. (A) Wild-type and *vps30Δ* cells expressing ATM (M) or ATZ (Z) were grown to saturation in the presence of methionine and diluted to an OD_{600} of 1.0, and colony immunoblots were performed. After immunoblotting for AT, the same blot was stripped and immunoblotted for the cytosolic protein G6PDH. (B) Quantitation of AT immunoblots from A. Three transformants were quantitated for each sample, and the mean background-corrected signal intensity is represented. Error bars indicate the standard deviation of the mean. (C) Mutant strains from plate 109 from the yeast deletion mutant collection were transformed with pATZ, and colony immunoblots were performed. Control spots are indicated by numbers: 1: wild type/ATM; 2: wild type/ATZ; 3: *vps30Δ*/ATZ. Solid boxes indicate the position of the *vps30Δ* strain within the plate, and the dashed boxes indicate the position of *met8Δ* strain, which is mutated for an enzyme involved in siroheme synthesis, and hence is defective for sulfite reductase activity and methionine biosynthesis. A small amount of *met8Δ* growth was supported by the residual methionine carried over from the starter culture during replica spotting. In A–C, IC + EC (total) indicates lysed colony immunoblots and EC (secreted) indicates unlysed colony blots. In C, the EC membrane was imaged using a more sensitive chemiluminescence reagent than the IC + EC membrane to allow comparison.

(Supporting Information, Figure S1), whereas the CPY signal in lysed colony immunoblots was similar between wild-type and mutant cells. This reflects the fact that the assay detects both the steady-state levels of intracellular CPY *and* the cumulative secreted levels of extracellular CPY.

Next, both the unlysed colony immunoblot (secreted AT) and the lysed colony immunoblot (total AT) were adapted to a microplate format, and the performance of the modified assay was tested (Figure 3C). Using the modified assay, the difference in ATM and ATZ secretion was readily apparent, as was the secretion phenotype of the *vps30Δ* strain (compare spots 1 and 2, and spot 2 to the box, respectively, in the EC panel of Fig 3C). The increased secretion of the *vps30Δ*

Table 1 Yeast deletion mutants exhibiting increased levels of secreted or total antitrypsin

Secreted ATZ ratio[a]	Total ATZ ratio[b]	Gene	Function	CPY secretion index[c]	UPR induction ratio[d]
2.7	1.8	*LAS21*	GPI core synthesis	<0.1	3.4
2.4	2.2	*VPS10/PEP1*	Endosomal sorting	1.0	–
2.3	2.0	*VPS5*	Endosomal sorting: Retromer	1.0	–
2.3	1.8	*VPS27*	Endosomal sorting: ESCRT–0	0.7	–
2.2	1.3	*CWC27*	Spliceosome associated	<0.1	–
2.1	2.0	*VPS17*	Endosomal sorting: Retromer	1.0	–
2.0	1.9	*MTQ1*	Methylation of translation release factor	<0.1[e]	–
2.0	1.3	*RPL16B*	Large ribosomal subunit	<0.1	–
1.8	1.5	*ROM2*	Cell-wall integrity pathway: Rho1/2 GEF	<0.1	–
1.8	2.0	*VAM10*	Homotypic vacuole fusion (overlaps *VPS5*)	0.9	–
1.8	1.6	*SWM2*	Unknown (adjacent to *VPS27*)	<0.1	–
1.7	1.6	*DID4*	Endosomal sorting: ESCRT III	0.4	–
1.6	1.4	*SNN1*	Endosomal sorting: BLOC-1 complex	<0.1	–
1.6	1.3	*TNA1*	Plasma membrane nicotinic acid permease	<0.1[e]	–
1.6	1.5	*SIF2*	Set3 complex HDAC	<0.1	–
1.6	2.2	*PMT2*	*O*-linked glycosylation	<0.1	3.0
1.5	1.2	*HOS2*	Set3 complex HDAC	<0.1	–
1.4	1.6	*MDM1*	Intermediate filament: organelle inheritance	0.1	–
1.3	1.5	*VPS51*	Endosomal sorting: GARP complex	0.5	1.9
0.6	1.7	*DBP7*	Ribosomal biogenesis	<0.1	–
0.2	2.0	*RPL42A*	Large ribosomal subunit	<0.1	–

GEF, guanine nucleotide exchange factor. HDAC, histone deacetylase. —, no significant induction of the UPR.
[a] Ratio of secreted ATZ for mutant compared to wild type.
[b] Ratio of total ATZ for mutant compared to wild type.
[c] From Schluter *et al.* (2008). Wild type has a CPY secretion index of 0, and the maximum level of CPY secretion corresponds to a secretion index of 1.
[d] From Jonikas *et al.* (2009). The ratio of basal expression from a UPR element reporter compared to a constitutive expression reporter.
[e] Strain that had a consensus CPY secretion index of <0.1, but for which the alpha mating-type mutant had a CPY secretion index of 1.

strain was not due to increased total protein, since a *met8Δ* strain showed increased total levels of ATZ, without an accompanying increase in ATZ secretion (dashed boxes). The phenotype of the *met8Δ* strain reflects our use of the *MET25* promoter to drive ATZ expression and is consistent with the fact that *met8* mutants exhibit increased *MET25* transcription (Thomas *et al.* 1990).

These tests demonstrated that unlysed colony immunoblots could be used to screen for mutants with increased ATZ secretion and that lysed colony immunoblots could be used to screen for mutants with increased intracellular ATZ levels in the absence of an ATZ secretion phenotype.

A screen of the yeast deletion mutant collection indicates a significant effect of endosomal sorting pathways on ATZ biogenesis

The yeast α-mating-type deletion mutant collection consists of 5132 single-gene deletion mutants, representing ~80% of the nonessential yeast genes. By using a modified yeast transformation protocol (see *Materials and Methods*), the ATZ expression construct was successfully transformed into >99% of the viable strains in the collection, and, for each plate of transformants, both unlysed and lysed colony immunoblots were performed. Strains showing increased ATZ secretion or increased total ATZ were identified by comparing each strain to the average signal for viable strains on the same plate. Strains that showed at least a threefold increase over the plate average were selected for a secondary screen, after excluding strains with known defects in methionine homeostasis and those strains mutated for ORFs classified as dubious.

Because data derived from comparisons to a plate average can be sensitive to outliers, and because some plates showed evidence of a peripheral position effect on colony growth (data not shown), the strains selected for secondary screening were re-arrayed in duplicate with a paired wild-type control and in an arrangement that prevented edge effects on colony growth. Lysed and unlysed colony immunoblots were again performed, and strains that showed an average increase >1.5-fold compared to wild type, with respect to either secreted or total ATZ levels, are listed in Table 1.

Most of the 21 mutants identified in this way exhibited increased ATZ secretion, and most of these strains also showed increased levels of total AT in the lysed colony immunoblots. However, since the extracellular contribution to immunoblot signal is cumulative (*i.e.*, it includes all AT secreted during the growth period), the intracellular contribution to the signal cannot be determined for strains with an increased secretion phenotype. Only two strains (*rpl42Δ* and *dbp7Δ*) showed increased intracellular ATZ levels without a corresponding increase in ATZ secretion. *RPL42A* and *DBP7*, respectively, encode a ribosomal protein and a putative RNA helicase involved in ribosome biogenesis (Daugeron and Linder 1998; Planta and Mager 1998). Since it is likely that these two genes affect some aspect of ATZ synthesis, they were not further investigated.

The Gene Ontology category that was most highly enriched in the list of 21 mutants was "endosome transport [GO:0016197]" ($P = 0.01$), and 8 of the mutants in the list (*pep1Δ/vps10Δ*; *vps5Δ*; *vps27Δ*; *vps17Δ*; *vam10Δ*; *did4Δ*; *snn1Δ*; *vps51Δ*) are known to have endosomal sorting defects. For example, the second-highest increase in ATZ secretion was exhibited by *pep1Δ/vps10Δ* (hereafter referred to as *vps10Δ*), which is mutated for the gene encoding a Golgi-to-endosome vacuolar protein sorting receptor (Bankaitis *et al.* 1986; Robinson *et al.* 1988; Rothman *et al.* 1989; Van Dyck *et al.* 1992; Marcusson *et al.* 1994). These results prompted us to compare the outcome of our screen with the results of a secretion screen performed with CPY (Schluter *et al.* 2008). CPY traffics to the vacuole via the endosome and is the canonical trafficking cargo of Vps10 (Marcusson *et al.* 1994). This comparison revealed that all 8 of the strains identified as having a likely endosomal sorting defect also showed increased secretion of CPY. However, 2 strains that showed increased ATZ secretion in this screen (*mtq1Δ* and *tna1Δ*) also showed increased CPY secretion (Schluter *et al.* 2008), but only in the strain from the α-mating-type collection (also used in this study). Therefore, the oversecretion phenotype of *mtq1Δ* and *tna1Δ* in these strains may be due to a cryptic mutation at a second site elsewhere in the genome.

Because induction of the unfolded protein response (UPR) can lead to increased secretion of select proteins (Belden and Barlowe 2001), we also examined whether any of our hits are known to induce the UPR (Jonikas *et al.* 2009). As shown in Table 1, three strains exhibited UPR induction, only one of which was also an endosomal sorting mutant (*vps51Δ*). The other two were *las21Δ*, which is deficient in glycosylphosphatidylinositol (GPI) core synthesis (Benachour *et al.* 1999), and *pmt2Δ*, which encodes an enzyme involved in *O*-linked protein glycosylation and ER quality control (Goder and Melero 2011). The *las21Δ* mutant is also known to secrete 2.2-fold more BiP (Copic *et al.* 2009), an ER chaperone that interacts with ATZ (Cabral *et al.* 2002; Schmidt and Perlmutter 2005).

The consistent effect of endosomal sorting mutations on ATZ secretion raised the question of whether the secretion of ATM is also affected in this class of mutants. We discovered that ATM secretion was unaffected in the *vps10Δ* strain under conditions similar to those used in the genome-wide screen (Table 2; $OD_{600} = 5$). However, because ATM is much more efficiently secreted than ATZ, we suspected that the ATM signal becomes saturated at the higher cell densities that were appropriate for assaying ATZ secretion. Indeed, when lower starting cell densities were used ($OD_{600} = 1$ and 0.2), a statistically significant increase in ATM secretion was observed in the *vps10Δ* strain. Therefore, Vps10 affects the secretion of both wild-type ATM and ATZ.

Table 2 Ratio of AT secreted in a *vps10Δ* strain compared to wild type

Starting density (OD_{600}/ml)[a]	AT variant	Secreted AT ratio (vps10Δ/WT)[b]	Standard deviation
5	ATM	1.1	0.1
	ATZ	2.4	0.6
1	ATM	1.7	0.1
	ATZ	3.1	0.3
0.2	ATM	2.8	0.1
	ATZ	3.4	0.2

[a] OD_{600} of the cell suspension spotted onto nitrocellulose membranes for colony immunoblot assay. Note that the genome-wide screen was performed using a stationary-phase cell suspension, which for most strains was an OD_{600} of ~5.
[b] Average ratio of secreted antitrypsin for *vps10Δ* compared to wild type as assessed from duplicate transformants.

AT is trafficked to the yeast vacuole via the Golgi

The results of the genome-wide screen revealed a surprising effect of the endosomal sorting pathway on AT secretion in yeast. This might arise from a direct effect of reduced trafficking of AT to the vacuole, and thus greater secretion, or it might be an indirect effect, caused by a change in the trafficking of another factor that affects AT secretion.

Consistent with the hypothesis that AT is trafficked to and degraded in the vacuole, we observed an accumulation of ATM and ATZ in the vacuole when immunofluorescence microscopy was performed in a *pep4Δ* strain, which has negligible vacuolar protease activity (Jones *et al.* 1982) (Figure 4A). This result demonstrates that some proportion of AT is degraded in the vacuole. However, since this experiment reflected steady-state levels of AT, the relative contribution of vacuolar proteases on AT turnover was unclear. Therefore, we performed pulse-chase degradation assays to directly monitor AT stability in the presence or absence of *PEP4* (Figure 4B). The data showed that, in wild-type cells, both ATM and ATZ were degraded to ~50% of their initial levels after 90 min. In contrast, in the *pep4Δ* strain, there was a marked increase in higher-molecular-weight AT species over time. When this higher-molecular-weight material was taken into account, AT was almost completely stabilized in the *pep4Δ* strain, indicating a significant vacuolar contribution to AT degradation (Figure 4C).

Soluble cargo from the ER can reach the vacuole either by autophagy or by the Golgi. ATZ in both yeast and mammals can be targeted for degradation by ERAD or by autophagy (Qu *et al.* 1996; Werner *et al.* 1996; Teckman and Perlmutter 2000; Kamimoto *et al.* 2006; Kruse *et al.* 2006), and in yeast the conversion of ATZ into a substrate for autophagy correlated with high levels of expression and growth on galactose (Kruse *et al.* 2006). However, the results from the genome-wide screen indicated that mutants impaired in endosomal sorting, but not autophagy, affected ATZ secretion. Notably, autophagy mutants were absent from hits from our screen (Table 1), and, when using the *MET25* expression system, we failed to observe ATZ stabilization in an *atg14Δ* mutant (Figure S2). Nevertheless, it has been shown that the endosomal sorting complex required for transport (ESCRT), which is a crucial component of the endosomal sorting machinery, is also involved in autophagosome homeostasis in higher organisms (Rusten and Stenmark 2009

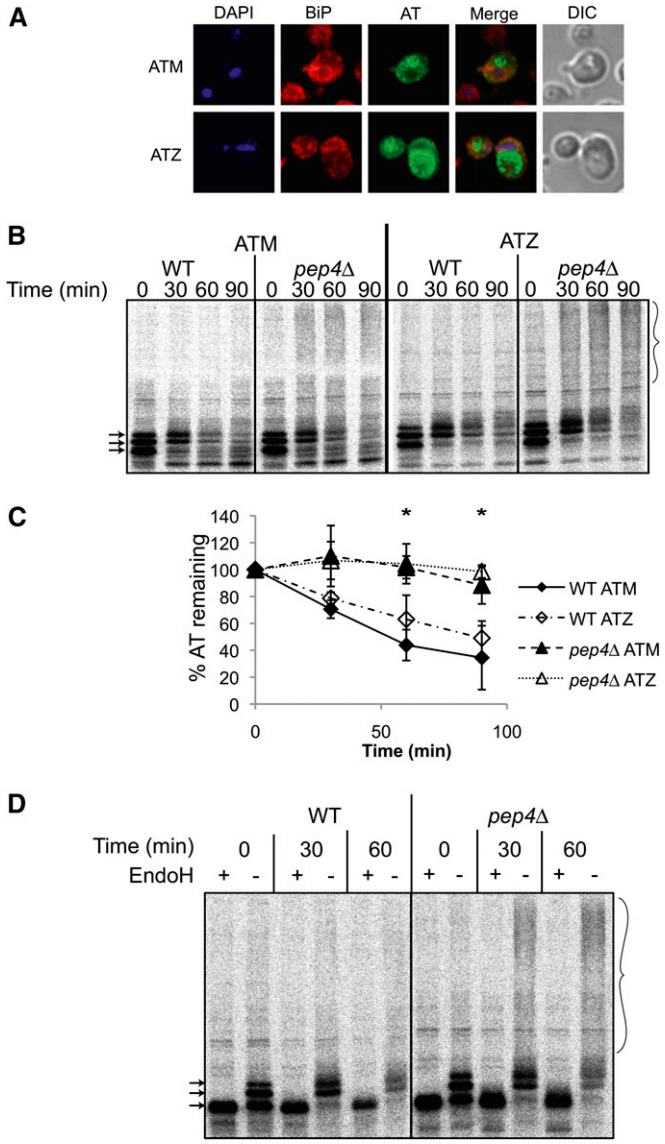

Figure 4 AT is trafficked to and degraded in the yeast vacuole. (A) Immunofluorescence microscopy of AT and BiP and nuclear localization by DAPI staining is shown in *pep4Δ* cells expressing ATM or ATZ. The position of the vacuole is visible in the DIC images and corresponds to the position of the majority of the AT signal. (B) AT pulse-chase analysis in wild-type and *pep4Δ* cells expressing ATM or ATZ. The large brace indicates the high-molecular-weight AT species that accumulate in the *pepΔ* strain. Arrows indicate an unglycosylated AT precursor (fastest migrating species) and two glycosylated forms of AT. (C) Quantification of the pulse-chase data from B. Three transformants were examined, and the averaged amount of AT remaining at each time point was expressed relative to the amount of AT present at the zero time point. Error bars represent the standard deviation. Asterisks indicate the time points at which there was a statistically significant ($P < 0.05$) difference in relative AT levels between wild-type and *pep4Δ* cells. (D) AT was immunoprecipitated from the samples examined in B and was incubated in the presence (+) or the absence (−) of Endo H and then analyzed by SDS-PAGE. The large brace indicates the high-molecular-weight AT species that accumulate in the *pep4Δ* strain. Arrows indicate an unglycosylated AT precursor (fastest migrating species) and two glycosylated forms of AT.

and references therein). Although two ESCRT mutants were identified in our screen (*vps27Δ*, *did4Δ*), these mutants have not been linked to autophagy function in yeast. In addition, other endosomal sorting mutants, such as *vps10Δ*, that are unlinked to autophagy in any organism showed similar phenotypes in our screen. To confirm that *vps10Δ* does not affect autophagy in yeast, we performed a GFP-Atg8 immunoblot autophagy assay (Kim *et al.* 2001) and found that starvation-induced autophagy was unaffected by the *vps10Δ* mutation (Figure S3).

In support of the hypothesis that AT reaches the vacuole via the Golgi, the higher-molecular-weight AT that accumulates in the absence of vacuolar protease activity was reminiscent of the hyper-*N*-glycosylated forms of secreted ATM (compare Figure 2A to Figure 4B). Indeed, the AT "smear" in the *pep4Δ* strain was Endo H-sensitive, confirming that these higher-molecular-weight species arise from hyper-*N*-glycosylation (Figure 4D), a modification that occurs only once a secreted protein has reached the Golgi in yeast. Taken together, these data indicate that a significant proportion of the AT that leaves the ER is diverted from the Golgi to the vacuole via the endosome. Moreover, these results suggest that, when endosomal sorting and degradation are compromised, the intracellular levels of AT rise, which in turn leads to increased secretion of AT.

Overexpression of the human homolog of Vps10 in rat hepatoma cells affects intracellular and extracellular AT levels

To investigate whether a similar AT disposal pathway might exist in mammalian cells, we examined whether overexpression of a human homolog of Vps10, known as sortilin, also affected ATZ biogenesis. Sortilin is an intracellular and endocytic sorting receptor that plays an established role in trafficking specific cargo proteins to the lysosome from the Golgi and the plasma membrane (Canuel *et al.* 2009; Hermey 2009; Strong and Rader 2012), but has not previously been implicated in the trafficking of AT. Sortilin consists of an extracellular domain that is homologous to yeast Vps10 and a cytoplasmic domain bearing two endosome/lysosome sorting motifs—a dileucine and a tyrosine-containing motif (Nielsen *et al.* 2001).

To investigate whether sortilin function affects AT trafficking, we used rat hepatoma cell lines (McArdle RH-7777) that stably express either sortilin (Sort) or a mutant version of sortilin in which key residues in the dileucine and tyrosine (YXXϕ) sorting motifs in the cytoplasmic domain have been mutated to alanine (Sort.LAYA) (Strong *et al.* 2012). It was previously shown that Sort.LAYA is aberrantly localized to the plasma membrane and unable to function in Golgi-to-endosome sorting. To examine the effect of overexpressing Sort and Sort.LAYA on AT biogenesis, we transiently transfected these cell lines with human ATM and ATZ C-terminally fused with a FLAG and a tetracysteine (TC) tag and then performed a pulse-chase analysis to quantify IC and EC AT-FLAG.

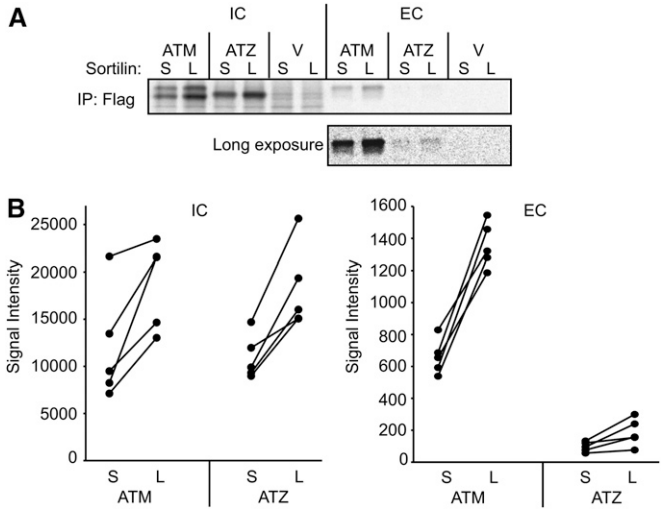

Figure 5 Overexpression of the human homolog of Vps10 sortilin in rat hepatoma cells affects intracellular and extracellular AT levels. (A) ATM-FLAG and ATZ-FLAG levels are decreased in McArdle RH-7777 cells that overexpress human wild-type sortilin (S) in comparison to cells that express the Sort.LAYA mis-sorting mutant version of sortilin (L). Cells stably expressing sortilin or Sort.LAYA were transiently transfected with pATM-FLAG, pATZ-FLAG, or the empty vector pRc/RSV ("V"). After 24 hr, cells were labeled for 20 min with ^{35}S-amino acids, followed by a 20-min chase. AT levels in cell lysates (IC) and media (EC) were analyzed by immunoprecipitation with anti-FLAG antibody and subjected to SDS-PAGE analysis. The low levels of ATZ-FLAG that were secreted after 20 min are detectable by enhancement of radiograph contrast and brightness (bottom). (B) Quantification from five independent replicates of this experiment is presented as a scatter plot showing individual sortilin *vs.* Sort.LAYA comparisons as paired data points. Each individual data point is represented by a dot, and comparisons across adjacent positions in a gel are connected by a line. The averaged data and statistical analysis for this experiment are shown in Table 3.

The AT-FLAG fusions could be specifically immunoprecipitated with either anti-FLAG or anti-AT (Figure S4). The FLAG-TC tag caused a decrease in electrophoretic mobility compared to untagged human AT, but otherwise showed behavior consistent with previous observations of AT in transfected cell lines. For example, after a chase period of 20 min, ATM-FLAG was present as two intracellular species, migrating at an apparent molecular mass of ~60 and ~64 kDa, whereas the secreted form of ATM-FLAG migrated as a single species with an apparent MW of ~64 kDa (Figure 5). This pattern corresponds closely to that seen for untagged ATM, in which cells initially synthesize an ~53-kDa glycosylated species, which is converted to an ~55-kDa form that bears complex-type oligosaccharides and is rapidly secreted (Lodish *et al.* 1983, 1987; Perlmutter *et al.* 1989). As expected, ATZ-FLAG was present intracellularly as a single band with an apparent MW similar to the faster-migrating ATM-FLAG species. That the behavior of AT-FLAG is substantially similar to that of untagged AT was also confirmed by the observation that only ~10% as much ATZ-FLAG was secreted compared to ATM-FLAG, and this ATZ-FLAG species had a similar electrophoretic mobility to ATM-FLAG. Together, these observations suggest that the trafficking of AT-FLAG is comparable to that of the untagged form.

Table 3 Ratio of AT-FLAG signal in cells expressing SORT.LAYA compared to cells expressing wild-type sortilin

Sample type[a]	AT variant	Mean ratio (Sort.LAYA/Sort)[b]	*P*-value[c]
IC	ATM	1.7	0.024
	ATZ	1.7	0.0024
EC	ATM	2.1	0.00098
	ATZ	1.9	0.012

[a] IC, intracellular; EC, extracellular.
[b] Mean ratio of AT-FLAG signal in Sort.LAYA cells compared to Sort cells.
[c] Estimate of the probability that the mean ratio is different from 1, as described in *Materials and Methods*.

Consistent with a role for sortilin in trafficking a fraction of AT-FLAG to the lysosome, overexpression of wild-type sortilin resulted in a statistically significant decrease of ~1.7-fold in intracellular ATM and ATZ levels when compared to ATM and ATZ levels when Sort.LAYA was expressed (Figure 5, A and B, and Table 3). Correspondingly, there was also a statistically significant, ~2-fold decrease in the amount of secreted ATM and ATZ. These data indicate that sortilin influences AT levels and secretion and furthermore are consistent with the hypothesis that sortilin promotes the degradation of AT from the late secretory pathway.

Discussion

If ATZ retained within hepatocytes is not efficiently degraded, its intracellular accumulation can result in liver disease (Perlmutter 2011). Perhaps not surprisingly, ATZ degradation has been implicated as one factor that may contribute to individual variation in susceptibility to ATD-associated liver disease. Two pathways, ERAD and autophagy, have been shown to degrade ER-localized ATZ (Qu *et al.* 1996; Werner *et al.* 1996; Teckman and Perlmutter 2000; Kamimoto *et al.* 2006; Kruse *et al.* 2006). The contributions of other degradation pathways have been hinted at, but remain undefined. For example, Sifers and colleagues reported that ATZ stably expressed in a murine hepatoma cell line was degraded by a proteasome-independent mechanism that was sensitive to tyrosine phosphatase inhibitors (Cabral *et al.* 2000). We hypothesized that a genome-wide screen, using the yeast model, might uncover novel routes through which ATZ is targeted for degradation and that, in turn, affect its secretion.

In the work reported in this article, the development and use of a yeast genome-wide deletion mutant screen revealed that a novel pathway of ATZ degradation operates in yeast, and we provide the first evidence that this pathway also affects ATZ levels and secretion in mammalian cells. Specifically, our screen identified yeast mutants that exhibited increased ATZ secretion, and the screen hits were significantly enriched for mutants impaired in endosomal sorting. Notably, each of the isolated mutants is known to aberrantly secrete the vacuolar protease CPY. In wild-type cells, CPY binds to the luminal domain of its sorting receptor Vps10 in a late-compartment of the Golgi (Marcusson *et al.* 1994).

The Vps10/CPY complex is then sorted into clathrin-coated vesicles and transported to the endosome (prevacuolar compartment), where CPY is released for transport to the vacuole while Vps10 is recycled to the Golgi (Seeger and Payne 1992; Piper *et al.* 1995; Cooper and Stevens 1996; Seaman *et al.* 1997; Chen and Graham 1998; Mullins and Bonifacino 2001). We found that mutations in the gene encoding Vps10, as well as those encoding members of the retromer complex, the GARP complex, and ESCRT subunits, which are required for Vps10 recycling, each result in increased secretion of AT. Together with our evidence that a significant portion of AT is degraded in the vacuole after obtaining Golgi-specific glycans, our data support a model in which AT can be diverted to the vacuole by Vps10. It is interesting to note that, even though Vps10 binds selectively to biosynthetic cargo like CPY, it was also shown to be required for the vacuolar sorting of a soluble, misfolded, heterologous protein, and it was hypothesized that Vps10 might be able to nonspecifically bind to extended polypeptides that result from partial misfolding (Hong *et al.* 1996; Jorgensen *et al.* 1999). This raised the possibility that Vps10 acts as a more general mediator of protein quality control in the Golgi. More recent work from Wang and Ng (2010) on the degradation of substrates subjected to Golgi quality control support a contribution of Vps10 during this process.

The genetic screen did not identify any mutants that modify ERAD, consistent with the data indicating that under these conditions the majority of AT degradation occurred in the vacuole. We suggest that this reflects the use of the *MET25* methionine-repressible promoter, which, as noted above, results in less metabolic stress; in other words, the ERAD requirement for AT degradation in yeast may be most prominent only during stress. We also did not observe a difference in the effect of the *vps10Δ* mutation on the secretion of ATM compared to ATZ, which we would predict if a Vps10-dependent pathway contributed specifically to the ATZ secretion defect. However, this does not rule out a role for Golgi quality control in AT sorting, especially if a significant amount of ATM reaches the Golgi in a misfolded conformation. In fact, it is generally accepted that correctly folded proteins can continue to exist in a dynamic equilibrium with unfolded states after exiting the ER (Powers *et al.* 2009), and ATM may fall into this class. Regardless, since the vacuolar sorting pathway clearly affected secretion and degradation of AT in yeast, and since this pathway is well conserved between yeast and mammals, we considered it an excellent candidate for a pathway that also influences AT trafficking in mammals.

As hypothesized, we found that both intracellular and secreted levels of human AT decreased in a rat hepatoma cell line that overexpresses a human Vps10 homolog, sortilin, compared to AT levels in a cell line the overexpresses a mutant form of sortilin. Sortilin is a member of the mammalian Vps10 domain family. All members of which bear a luminal domain that is homologous to the paired luminal domains of yeast Vps10 (Petersen *et al.* 1997; Hermey 2009). However, sortilin is the mammalian homolog with the most modular similarity to Vps10 (the other family members have additional luminal domains). Sortilin also has functions that are clearly analogous with those of Vps10, as evidenced by the lysosomal targeting of cathepsins (Canuel *et al.* 2008). In addition, sortilin binds a diverse range of intracellular and extracellular cargo (Nykjaer and Willnow 2012), which is suggestive of some flexibility in its binding determinants.

Although we cannot rule out an indirect effect of sortilin on altered levels of AT, our experiments suggest that sortilin is a candidate genetic modifier of AT degradation and secretion, and thus of ATZ-associated liver disease. Modulation of the endosomal sorting system, either genetically or therapeutically, may modify disease severity. It is important to note that modulators of autophagy did not similarly change the levels of secreted ATZ (Kamimoto *et al.* 2006). Interestingly, there is significant variation in liver-specific sortilin expression in human populations, and this variation is already known to have important clinical consequences. Specifically, a common genetic polymorphism associated with a >10-fold increased expression of sortilin in the liver correlates with both lower levels of serum low-density lipoprotein cholesterol (LDL-C) and a lower risk for cardiovascular disease (Samani *et al.* 2007; Kathiresan *et al.* 2008; Musunuru *et al.* 2010). This variant shows the strongest association with LDL-C levels of any locus in the genome (Teslovich *et al.* 2010). Although the directionality of the relationship between sortilin expression and circulating LDL-C is under debate, the data are consistent with an effect of sortilin on the hepatic secretion, degradation, or uptake of lipoproteins (Kjolby *et al.* 2010; Linsel-Nitschke *et al.* 2010; Musunuru *et al.* 2010; reviewed in Tall and Ai 2011; Willnow *et al.* 2011; Strong and Rader 2012). Given the diversity of sortilin cargo, it is likely that other proteins secreted by hepatocytes are also affected by this polymorphism. We propose that AT may be one such protein, and it remains to be discovered whether polymorphisms affecting sortilin expression are associated with different clinical outcomes of individuals afflicted with antitrypsin deficiency.

Acknowledgments

We thank Daniel Rader, Judith Frydman, Daniel Klionsky, Mark Rose, Suresh Subramani, Gary Silverman, Steven Pak, Tunda Hidvegi, Souvik Chakraborty, Alanna Strong, Charles Guo, Ana Tuyama, David Lomas, Maria Elena Miranda Banos, and Simon Watkins for reagents and advice. We also acknowledge the assistance of the Center for Biologic Imaging at the University of Pittsburgh [Pittsburgh Center for Kidney Research, National Institutes of Health (NIH) grant DK79307]. C.L.G. was supported by an Alpha-1 Foundation Postdoctoral Fellowship, an Australian Research Council International Fellowship (LX 0989187), and an American–Australian Association scholarship. This work was supported by NIH grant GM75061 to J.L.B. and by grant HL58541 to E.A.F and J.L.B.

Literature Cited

Adams, A., D. E. Gottschling, C. A. Kaiser, and T. Stearns, 1997 Media and stock preservation, pp. 145–160 in *Methods in Yeast Genetics: A Cold Spring Harbor Laboratory Course Manual*. Cold Spring Harbor Laboratory Press, Cold Spring Harbor, NY.

Amberg, D. C., D. J. Burke, and J. N. Strathern, 2005 Yeast immunofluorescence, pp. 149–152 in *Methods in Yeast Genetics: A Cold Spring Harbor Laboratory Course Manual*. Cold Spring Harbor Laboratory Press, Cold Spring Harbor, NY.

Bankaitis, V. A., L. M. Johnson, and S. D. Emr, 1986 Isolation of yeast mutants defective in protein targeting to the vacuole. Proc. Natl. Acad. Sci. USA 83: 9075–9079.

Bathurst, I. C., J. Travis, P. M. George, and R. W. Carrell, 1984 Structural and functional characterization of the abnormal Z alpha 1-antitrypsin isolated from human liver. FEBS Lett. 177: 179–183.

Bathurst, I. C., D. M. Errington, R. C. Foreman, J. D. Judah, and R. W. Carrell, 1985 Human Z alpha 1-antitrypsin accumulates intracellularly and stimulates lysosomal activity when synthesised in the Xenopus oocyte. FEBS Lett. 183: 304–308.

Belden, W. J., and C. Barlowe, 2001 Deletion of yeast p24 genes activates the unfolded protein response. Mol. Biol. Cell 12: 957–969.

Benachour, A., G. Sipos, I. Flury, F. Reggiori, E. Canivenc-Gansel *et al.*, 1999 Deletion of GPI7, a yeast gene required for addition of a side chain to the glycosylphosphatidylinositol (GPI) core structure, affects GPI protein transport, remodeling, and cell wall integrity. J. Biol. Chem. 274: 15251–15261.

Bernales, S., K. L. McDonald, and P. Walter, 2006 Autophagy counterbalances endoplasmic reticulum expansion during the unfolded protein response. PLoS Biol. 4: e423.

Brachmann, C. B., A. Davies, G. J. Cost, E. Caputo, J. Li *et al.*, 1998 Designer deletion strains derived from Saccharomyces cerevisiae S288C: a useful set of strains and plasmids for PCR-mediated gene disruption and other applications. Yeast 14: 115–132.

Brodsky, J. L., and R. Schekman, 1993 A Sec63p-Bip complex from yeast is required for protein translocation in a reconstituted proteoliposome. J. Cell Biol. 123: 1355–1363.

Brodsky, J. L., S. Hamamoto, D. Feldheim, and R. Schekman, 1993 Reconstitution of protein translocation from solubilized yeast membranes reveals topologically distinct roles for BiP and cytosolic Hsc70. J. Cell Biol. 120: 95–102.

Brodsky, J. L., E. D. Werner, M. E. Dubas, J. L. Goeckeler, K. B. Kruse *et al.*, 1999 The requirement for molecular chaperones during endoplasmic reticulum-associated protein degradation demonstrates that protein export and import are mechanistically distinct. J. Biol. Chem. 274: 3453–3460.

Cabral, C. M., P. Choudhury, Y. Liu, and R. N. Sifers, 2000 Processing by endoplasmic reticulum mannosidases partitions a secretion-impaired glycoprotein into distinct disposal pathways. J. Biol. Chem. 275: 25015–25022.

Cabral, C. M., Y. Liu, K. W. Moremen, and R. N. Sifers, 2002 Organizational diversity among distinct glycoprotein endoplasmic reticulum-associated degradation programs. Mol. Biol. Cell 13: 2639–2650.

Canuel, M., A. Korkidakis, K. Konnyu, and C. R. Morales, 2008 Sortilin mediates the lysosomal targeting of cathepsins D and H. Biochem. Biophys. Res. Commun. 373: 292–297.

Canuel, M., Y. Libin, and C. R. Morales, 2009 The interactomics of sortilin: an ancient lysosomal receptor evolving new functions. Histol. Histopathol. 24: 481–492.

Carlson, J. A., B. B. Rogers, R. N. Sifers, M. J. Finegold, S. M. Clift *et al.*, 1989 Accumulation of PiZ alpha 1-antitrypsin causes liver damage in transgenic mice. J. Clin. Invest. 83: 1183–1190.

Chappell, S., T. Guetta-Baranes, N. Hadzic, R. Stockley, and N. Kalsheker, 2009 Polymorphism in the endoplasmic reticulum mannosidase I (MAN1B1) gene is not associated with liver disease in individuals homozygous for the Z variant of the alpha1-antitrypsin protease inhibitor (PiZZ individuals). Hepatology 50: 1315; author reply 1315–1316.

Chen, C. Y., and T. R. Graham, 1998 An arf1Delta synthetic lethal screen identifies a new clathrin heavy chain conditional allele that perturbs vacuolar protein transport in *Saccharomyces cerevisiae*. Genetics 150: 577–589.

Cooper, A. A., and T. H. Stevens, 1996 Vps10p cycles between the late-Golgi and prevacuolar compartments in its function as the sorting receptor for multiple yeast vacuolar hydrolases. J. Cell Biol. 133: 529–541.

Copic, A., M. Dorrington, S. Pagant, J. Barry, M. C. Lee *et al.*, 2009 Genomewide analysis reveals novel pathways affecting endoplasmic reticulum homeostasis, protein modification and quality control. Genetics 182: 757–769.

Daugeron, M. C., and P. Linder, 1998 Dbp7p, a putative ATP-dependent RNA helicase from Saccharomyces cerevisiae, is required for 60S ribosomal subunit assembly. RNA 4: 566–581.

de Serres, F. J., I. Blanco, and E. Fernandez-Bustillo, 2007 PI S and PI Z alpha-1 antitrypsin deficiency worldwide. A review of existing genetic epidemiological data. Monaldi Arch. Chest Dis. 67: 184–208.

de Serres, F. J., I. Blanco, and E. Fernandez-Bustillo, 2010 Ethnic differences in alpha-1 antitrypsin deficiency in the United States of America. Ther. Adv. Respir. Dis. 4: 63–70.

Dycaico, M. J., S. G. Grant, K. Felts, W. S. Nichols, S. A. Geller *et al.*, 1988 Neonatal hepatitis induced by alpha 1-antitrypsin: a transgenic mouse model. Science 242: 1409–1412.

Eriksson, S., 1987 Alpha 1-antitrypsin deficiency and liver cirrhosis in adults. An analysis of 35 Swedish autopsied cases. Acta Med. Scand. 221: 461–467.

Errington, D. M., I. C. Bathurst, and R. W. Carrell, 1985 Human alpha 1-antitrypsin expression in Xenopus oocytes. Secretion of the normal (PiM) and abnormal (PiZ) forms. Eur. J. Biochem. 153: 361–365.

Esmon, B., P. Novick, and R. Schekman, 1981 Compartmentalized assembly of oligosaccharides on exported glycoproteins in yeast. Cell 25: 451–460.

Foreman, R. C., J. D. Judah, and A. Colman, 1984 Xenopus oocytes can synthesise but do not secrete the Z variant of human alpha 1-antitrypsin. FEBS Lett. 168: 84–88.

Gelling, C. L., and J. L. Brodsky, 2010 Mechanisms underlying the cellular clearance of antitrypsin Z: lessons from yeast expression systems. Proc. Am. Thorac. Soc. 7: 363–367.

Giaever, G., A. M. Chu, L. Ni, C. Connelly, L. Riles *et al.*, 2002 Functional profiling of the Saccharomyces cerevisiae genome. Nature 418: 387–391.

Gietz, D. R., R. A. Woods, C. F. Guthrie, and G. R. Fink, 2002 Transformation of yeast by lithium acetate/single-stranded carrier DNA/polyethylene glycol method. Methods Enzymol. 350: 87.

Goder, V., and A. Melero, 2011 Protein O-mannosyltransferases participate in ER protein quality control. J. Cell Sci. 124: 144–153.

Hermey, G., 2009 The Vps10p-domain receptor family. Cell. Mol. Life Sci. 66: 2677–2689.

Hidvegi, T., M. Ewing, P. Hale, C. Dippold, C. Beckett *et al.*, 2010 An autophagy-enhancing drug promotes degradation of mutant alpha1-antitrypsin Z and reduces hepatic fibrosis. Science 329: 229–232.

Hong, E., A. R. Davidson, and C. A. Kaiser, 1996 A pathway for targeting soluble misfolded proteins to the yeast vacuole. J. Cell Biol. 135: 623–633.

Hosokawa, N., L. O. Tremblay, Z. You, A. Herscovics, I. Wada *et al.*, 2003 Enhancement of endoplasmic reticulum (ER) degradation of misfolded Null Hong Kong alpha1-antitrypsin by human ER mannosidase I. J. Biol. Chem. 278: 26287–26294.

Janus, E. D., N. T. Phillips, and R. W. Carrell, 1985 Smoking, lung function, and alpha 1-antitrypsin deficiency. Lancet 1: 152–154.

Jones, E. W., G. S. Zubenko, and R. R. Parker, 1982 PEP4 gene function is required for expression of several vacuolar hydrolases in *Saccharomyces cerevisiae*. Genetics 102: 665–677.

Jonikas, M. C., S. R. Collins, V. Denic, E. Oh, E. M. Quan *et al.*, 2009 Comprehensive characterization of genes required for protein folding in the endoplasmic reticulum. Science 323: 1693–1697.

Jorgensen, M. U., S. D. Emr, and J. R. Winther, 1999 Ligand recognition and domain structure of Vps10p, a vacuolar protein sorting receptor in Saccharomyces cerevisiae. Eur. J. Biochem. 260: 461–469.

Kamimoto, T., S. Shoji, T. Hidvegi, N. Mizushima, K. Umebayashi *et al.*, 2006 Intracellular inclusions containing mutant alpha1-antitrypsin Z are propagated in the absence of autophagic activity. J. Biol. Chem. 281: 4467–4476.

Kathiresan, S., O. Melander, C. Guiducci, A. Surti, N. P. Burtt *et al.*, 2008 Six new loci associated with blood low-density lipoprotein cholesterol, high-density lipoprotein cholesterol or triglycerides in humans. Nat. Genet. 40: 189–197.

Kim, J., W. P. Huang, and D. J. Klionsky, 2001 Membrane recruitment of Aut7p in the autophagy and cytoplasm to vacuole targeting pathways requires Aut1p, Aut2p, and the autophagy conjugation complex. J. Cell Biol. 152: 51–64.

Kimpen, J., E. Bosmans, and J. Raus, 1988 Neonatal screening for alpha-1-antitrypsin deficiency. Eur. J. Pediatr. 148: 86–88.

Kjolby, M., O. M. Andersen, T. Breiderhoff, A. W. Fjorback, K. M. Pedersen *et al.*, 2010 Sort1, encoded by the cardiovascular risk locus 1p13.3, is a regulator of hepatic lipoprotein export. Cell Metab. 12: 213–223.

Kruse, K. B., J. L. Brodsky, and A. A. McCracken, 2006 Characterization of an ERAD gene as VPS30/ATG6 reveals two alternative and functionally distinct protein quality control pathways: one for soluble Z variant of human alpha-1 proteinase inhibitor (A1PiZ) and another for aggregates of A1PiZ. Mol. Biol. Cell 17: 203–212.

Lin, L., B. Schmidt, J. Teckman, and D. H. Perlmutter, 2001 A naturally occurring nonpolymerogenic mutant of alpha 1-antitrypsin characterized by prolonged retention in the endoplasmic reticulum. J. Biol. Chem. 276: 33893–33898.

Linsel-Nitschke, P., J. Heeren, Z. Aherrahrou, P. Bruse, C. Gieger *et al.*, 2010 Genetic variation at chromosome 1p13.3 affects sortilin mRNA expression, cellular LDL-uptake and serum LDL levels which translates to the risk of coronary artery disease. Atherosclerosis 208: 183–189.

Lodish, H. F., N. Kong, M. Snider, and G. J. Strous, 1983 Hepatoma secretory proteins migrate from rough endoplasmic reticulum to Golgi at characteristic rates. Nature 304: 80–83.

Lodish, H. F., N. Kong, S. Hirani, and J. Rasmussen, 1987 A vesicular intermediate in the transport of hepatoma secretory proteins from the rough endoplasmic reticulum to the Golgi complex. J. Cell Biol. 104: 221–230.

Lomas, D. A., D. L. Evans, J. T. Finch, and R. W. Carrell, 1992 The mechanism of Z alpha 1-antitrypsin accumulation in the liver. Nature 357: 605–607.

Marcusson, E. G., B. F. Horazdovsky, J. L. Cereghino, E. Gharakhanian, and S. D. Emr, 1994 The sorting receptor for yeast vacuolar carboxypeptidase Y is encoded by the VPS10 gene. Cell 77: 579–586.

McCracken, A. A., and K. B. Kruse, 1993 Selective protein degradation in the yeast exocytic pathway. Mol. Biol. Cell 4: 729–736.

McCracken, A. A., I. V. Karpichev, J. E. Ernaga, E. D. Werner, A. G. Dillin *et al.*, 1996 Yeast mutants deficient in ER-associated degradation of the Z variant of alpha-1-protease inhibitor. Genetics 144: 1355–1362.

Mullins, C., and J. S. Bonifacino, 2001 Structural requirements for function of yeast GGAs in vacuolar protein sorting, alpha-factor maturation, and interactions with clathrin. Mol. Cell. Biol. 21: 7981–7994.

Mumberg, D., R. Muller, and M. Funk, 1994 Regulatable promoters of Saccharomyces cerevisiae: comparison of transcriptional activity and their use for heterologous expression. Nucleic Acids Res. 22: 5767–5768.

Musunuru, K., A. Strong, M. Frank-Kamenetsky, N. E. Lee, T. Ahfeldt *et al.*, 2010 From noncoding variant to phenotype via SORT1 at the 1p13 cholesterol locus. Nature 466: 714–719.

Nielsen, M. S., P. Madsen, E. I. Christensen, A. Nykjaer, J. Gliemann *et al.*, 2001 The sortilin cytoplasmic tail conveys Golgi-endosome transport and binds the VHS domain of the GGA2 sorting protein. EMBO J. 20: 2180–2190.

Nykjaer, A., and T. E. Willnow, 2012 Sortilin: a receptor to regulate neuronal viability and function. Trends Neurosci. 35: 261–270.

Palmer, E. A., K. B. Kruse, S. W. Fewell, S. M. Buchanan, J. L. Brodsky *et al.*, 2003 Differential requirements of novel A1PiZ degradation deficient (ADD) genes in ER-associated protein degradation. J. Cell Sci. 116: 2361–2373.

Pan, S., and R. N. Sifers, 2009 Reply. Hepatology 50: 1315–1316.

Pan, S., L. Huang, J. McPherson, D. Muzny, F. Rouhani *et al.*, 2009 Single nucleotide polymorphism-mediated translational suppression of endoplasmic reticulum mannosidase I modifies the onset of end-stage liver disease in alpha1-antitrypsin deficiency. Hepatology 50: 275–281.

Perlmutter, D. H., 2011 Alpha-1-antitrypsin deficiency: importance of proteasomal and autophagic degradative pathways in disposal of liver disease-associated protein aggregates. Annu. Rev. Med. 62: 333–345.

Perlmutter, D. H., R. M. Kay, F. S. Cole, T. H. Rossing, D. Van Thiel *et al.*, 1985a A selective defect in secretion of alpha 1-proteinase inhibitor PiZZ demonstrated in surrogate and primary extrahepatic cell culture. Trans. Assoc. Am. Physicians 98: 47–54.

Perlmutter, D. H., R. M. Kay, F. S. Cole, T. H. Rossing, D. Van Thiel *et al.*, 1985b The cellular defect in alpha 1-proteinase inhibitor (alpha 1-PI) deficiency is expressed in human monocytes and in Xenopus oocytes injected with human liver mRNA. Proc. Natl. Acad. Sci. USA 82: 6918–6921.

Perlmutter, D. H., L. T. May, and P. B. Sehgal, 1989 Interferon beta 2/interleukin 6 modulates synthesis of alpha 1-antitrypsin in human mononuclear phagocytes and in human hepatoma cells. J. Clin. Invest. 84: 138–144.

Petersen, C. M., M. S. Nielsen, A. Nykjaer, L. Jacobsen, N. Tommerup *et al.*, 1997 Molecular identification of a novel candidate sorting receptor purified from human brain by receptor-associated protein affinity chromatography. J. Biol. Chem. 272: 3599–3605.

Piper, R. C., A. A. Cooper, H. Yang, and T. H. Stevens, 1995 VPS27 controls vacuolar and endocytic traffic through a prevacuolar compartment in Saccharomyces cerevisiae. J. Cell Biol. 131: 603–617.

Planta, R. J., and W. H. Mager, 1998 The list of cytoplasmic ribosomal proteins of Saccharomyces cerevisiae. Yeast 14: 471–477.

Powers, E. T., R. I. Morimoto, A. Dillin, J. W. Kelly, and W. E. Balch, 2009 Biological and chemical approaches to diseases of proteostasis deficiency. Annu. Rev. Biochem. 78: 959–991.

Qu, D., J. H. Teckman, S. Omura, and D. H. Perlmutter, 1996 Degradation of a mutant secretory protein, alpha1-antitrypsin Z, in the endoplasmic reticulum requires proteasome activity. J. Biol. Chem. 271: 22791–22795.

Robinson, J. S., D. J. Klionsky, L. M. Banta, and S. D. Emr, 1988 Protein sorting in Saccharomyces cerevisiae: isolation of mutants defective in the delivery and processing of multiple vacuolar hydrolases. Mol. Cell. Biol. 8: 4936–4948.

Rothman, J. H., I. Howald, and T. H. Stevens, 1989 Characterization of genes required for protein sorting and vacuolar function in the yeast Saccharomyces cerevisiae. EMBO J. 8: 2057–2065.

Rusten, T. E., and H. Stenmark, 2009 How do ESCRT proteins control autophagy? J. Cell Sci. 122: 2179–2183.

Samani, N. J., J. Erdmann, A. S. Hall, C. Hengstenberg, M. Mangino *et al.*, 2007 Genomewide association analysis of coronary artery disease. N. Engl. J. Med. 357: 443–453.

Schluter, C., K. K. Lam, J. Brumm, B. W. Wu, M. Saunders *et al.*, 2008 Global analysis of yeast endosomal transport identifies the vps55/68 sorting complex. Mol. Biol. Cell 19: 1282–1294.

Schmidt, B. Z., and D. H. Perlmutter, 2005 Grp78, Grp94, and Grp170 interact with alpha1-antitrypsin mutants that are retained in the endoplasmic reticulum. Am. J. Physiol. Gastrointest. Liver Physiol. 289: G444–G455.

Seaman, M. N., E. G. Marcusson, J. L. Cereghino, and S. D. Emr, 1997 Endosome to Golgi retrieval of the vacuolar protein sorting receptor, Vps10p, requires the function of the VPS29, VPS30, and VPS35 gene products. J. Cell Biol. 137: 79–92.

Seeger, M., and G. S. Payne, 1992 A role for clathrin in the sorting of vacuolar proteins in the Golgi complex of yeast. EMBO J. 11: 2811–2818.

Silverman, E. K., J. P. Miletich, J. A. Pierce, L. A. Sherman, S. K. Endicott *et al.*, 1989 Alpha-1-antitrypsin deficiency. High prevalence in the St. Louis area determined by direct population screening. Am. Rev. Respir. Dis. 140: 961–966.

Spence, W. C., J. E. Morris, K. Pass, and P. D. Murphy, 1993 Molecular confirmation of alpha 1-antitrypsin genotypes in newborn dried blood specimens. Biochem. Med. Metab. Biol. 50: 233–240.

Stirling, C. J., J. Rothblatt, M. Hosobuchi, R. Deshaies, and R. Schekman, 1992 Protein translocation mutants defective in the insertion of integral membrane-proteins into the endoplasmic-reticulum. Mol. Biol. Cell 3: 129–142.

Strong, A., and D. J. Rader, 2012 Sortilin as a regulator of lipoprotein metabolism. Curr. Atheroscler. Rep. 14: 211–218.

Strong, A., Q. Ding, A. C. Edmondson, J. S. Millar, K. V. Sachs *et al.*, 2012 Hepatic sortilin regulates both apolipoprotein B secretion and LDL catabolism. J. Clin. Invest. 122: 2807–2816.

Sveger, T., 1976 Liver disease in alpha1-antitrypsin deficiency detected by screening of 200,000 infants. N. Engl. J. Med. 294: 1316–1321.

Tall, A. R., and D. Ai, 2011 Sorting out sortilin. Circ. Res. 108: 158–160.

Teckman, J. H., and D. H. Perlmutter, 2000 Retention of mutant alpha(1)-antitrypsin Z in endoplasmic reticulum is associated with an autophagic response. Am. J. Physiol. Gastrointest. Liver Physiol. 279: G961–G974.

Teslovich, T. M., K. Musunuru, A. V. Smith, A. C. Edmondson, I. M. Stylianou *et al.*, 2010 Biological, clinical and population relevance of 95 loci for blood lipids. Nature 466: 707–713.

Thomas, D., R. Barbey, and Y. Surdin-Kerjan, 1990 Gene-enzyme relationship in the sulfate assimilation pathway of Saccharomyces cerevisiae. Study of the 3′-phosphoadenylylsulfate reductase structural gene. J. Biol. Chem. 265: 15518–15524.

Van Dyck, L., B. Purnelle, J. Skala, and A. Goffeau, 1992 An 11.4 kb DNA segment on the left arm of yeast chromosome II carries the carboxypeptidase Y sorting gene PEP1, as well as ACH1, FUS3 and a putative ARS. Yeast 8: 769–776.

von der Haar, T., 2007 Optimized protein extraction for quantitative proteomics of yeasts. PLoS ONE 2: e1078.

Wang, S., and D. T. Ng, 2010 Evasion of endoplasmic reticulum surveillance makes Wsc1p an obligate substrate of Golgi quality control. Mol. Biol. Cell 21: 1153–1165.

Werner, E. D., J. L. Brodsky, and A. A. McCracken, 1996 Proteasome-dependent endoplasmic reticulum-associated protein degradation: an unconventional route to a familiar fate. Proc. Natl. Acad. Sci. USA 93: 13797–13801.

Willnow, T. E., M. Kjolby, and A. Nykjaer, 2011 Sortilins: new players in lipoprotein metabolism. Curr. Opin. Lipidol. 22: 79–85.

Winzeler, E. A., D. D. Shoemaker, A. Astromoff, H. Liang, K. Anderson *et al.*, 1999 Functional characterization of the S. cerevisiae genome by gene deletion and parallel analysis. Science 285: 901–906.

Wu, Y., I. Whitman, E. Molmenti, K. Moore, P. Hippenmeyer *et al.*, 1994 A lag in intracellular degradation of mutant alpha 1-antitrypsin correlates with the liver disease phenotype in homozygous PiZZ alpha 1-antitrypsin deficiency. Proc. Natl. Acad. Sci. USA 91: 9014–9018.

Wu, Y., M. T. Swulius, K. W. Moremen, and R. N. Sifers, 2003 Elucidation of the molecular logic by which misfolded alpha 1-antitrypsin is preferentially selected for degradation. Proc. Natl. Acad. Sci. USA 100: 8229–8234.

Yorimitsu, T., U. Nair, Z. Yang, and D. J. Klionsky, 2006 Endoplasmic reticulum stress triggers autophagy. J. Biol. Chem. 281: 30299–30304.

Communicating editor: M. D. Rose

GENETICS

Supporting Information
http://www.genetics.org/lookup/suppl/doi:10.1534/genetics.112.143487/-/DC1

The Endosomal Protein-Sorting Receptor Sortilin Has a Role in Trafficking α-1 Antitrypsin

Cristy L. Gelling, Ian W. Dawes, David H. Perlmutter, Edward A. Fisher, and Jeffrey L. Brodsky

DOI: 10.1534/genetics.112.143487

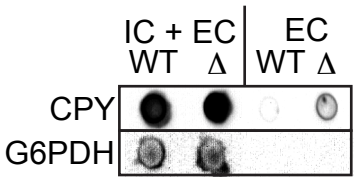

Figure S1. The CPY secretion phenotype of a *vps30*Δ strain can be detected by the colony immunoblot procedure.
Wild-type and *vps30*Δ (indicated by Δ) cells were grown to saturation in the presence of methionine, diluted to an OD_{600} of 1 and CPY colony immunoblots were performed as outlined in the Materials and Methods using an anti-CPY or anti-G6PDH antibody. G6PDH is a cytosolic enzyme. IC + EC refers to total intracellular and extracellular signal. EC refers to extracellular signal only.

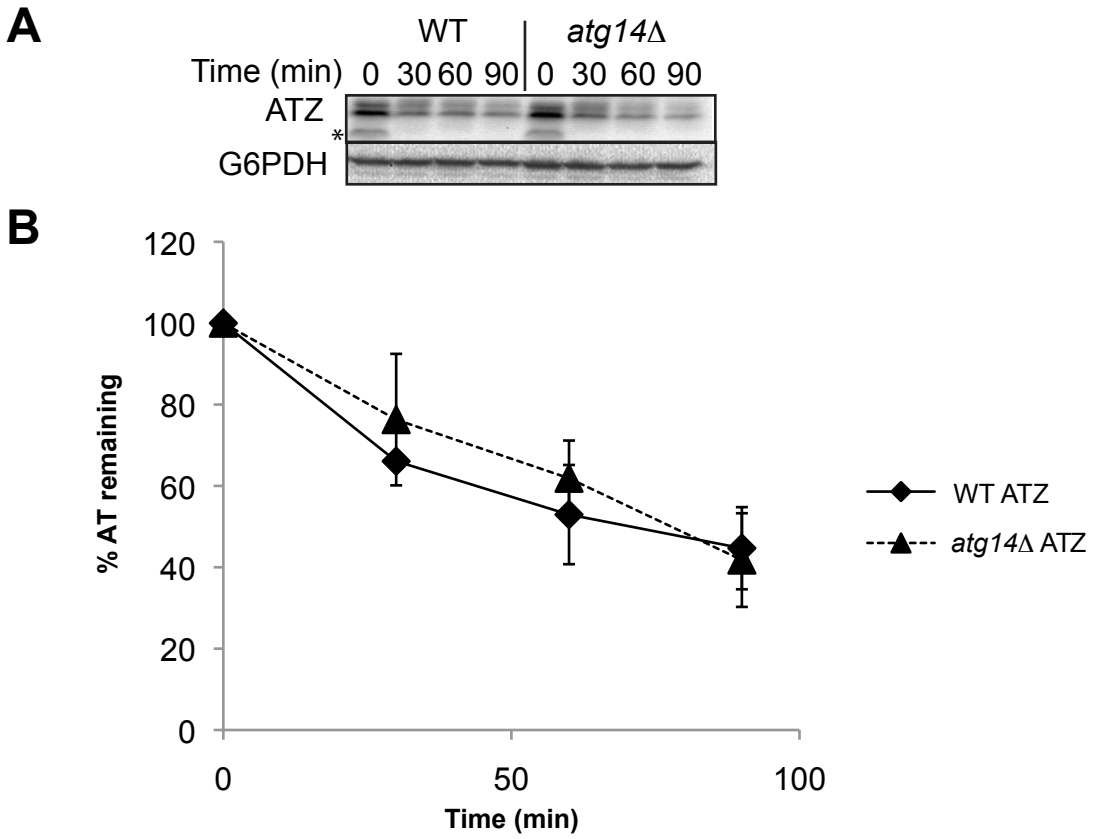

Figure S2. Degradation of ATZ is not affected in an autophagy mutant.
(A) The degradation of ATZ was compared between wild-type and the autophagy-defective *atg14*Δ mutant by cycloheximide chase. Cells were grown to log phase and protein synthesis halted by addition of cycloheximide. Samples were taken at the indicated time points and AT levels were analyzed by immunoblot. A representative immunoblot is shown. The asterisk indicates the position of a non-membrane-protected AT species (see Fig 1). (B) Quantification of data represented in part A. Three transformants were assayed for each strain and the amount of AT present at each time point was expressed as an average relative to the amount present at zero time. Error bars represent the standard deviation.

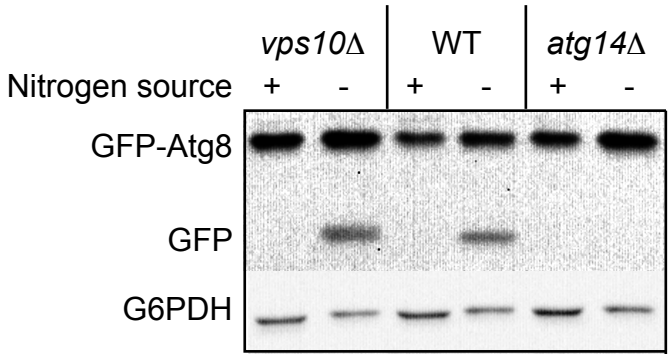

Figure S3. Autophagy is not impaired in a *vps10*Δ mutant.
Wild-type, *vps10*Δ, and *atg14*Δ cells were grown to exponential phase and either immediately harvested (+ nitrogen source) or autophagy was induced by nitrogen starvation for 4 h (- nitrogen source). GFP-Atg8 and the smaller vacuolar degradation product (GFP), which is indicative of autophagy, were detected by immunoblotting for GFP. G6PDH was used as a loading control.

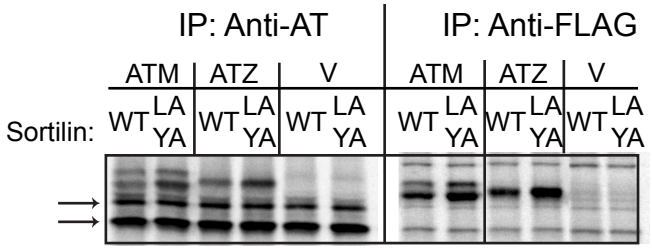

Figure S4. AT-FLAG can be immunoprecipitated by either anti-AT or anti-FLAG. Cells stably expressing Sortilin or Sort.LAYA were transiently transfected with pATM-FLAG (ATM), pATZ-FLAG (ATZ) or the empty vector pRc/RSV (V). After 24 h, cells were labeled for 20 min with ^{35}S-amino acids, followed by a 20 min chase. AT levels in cell lysates were analyzed by immunoprecipitation with either anti-FLAG or anti-AT and subject to SDS-PAGE analysis. Arrowheads denote the positions of non-specific species.